Nanofiltration membranes for salt and dye filtration: effect of membrane properties on performances

Meltem Ağtaş, Türkan Ormancı-Acar, Başak Keskin, Türker Türken and İsmail Koyuncu

ABSTRACT

In this study, commercial nanofiltration membranes (Toray, NF 270, Desal 5 L) were characterized by Fourier transform infrared spectroscopy, scanning electron microscopy, optical profilometry, contact angle, mechanical strength and zeta potential measurements. Filtration performance tests were conducted with distilled water, $MgSO_4$ solution and synthetic dye solutions, respectively. Among three commercial membranes, the Toray membrane was thought to be better choice. Additional experiments were carried out for a more detailed characterization of the selected membrane. Therefore, firstly, flux and removal efficiency was monitored by using dye solutions at different pH values, and then experiments were carried out to observe the effect of different temperatures. Also, another filtration test with NaCl solution was performed for the Toray membrane. As the main purpose of this study, we aimed to establish a significant correlation between the structural properties of membranes and their performances. In light of the results obtained, it was observed that the contact angle, mechanical strength and surface roughness values of the membrane significantly affected the membrane performance. It was concluded that the most important parameter in dye removal was the zeta potential. As a result of this work, a data set of commercial membranes was created and is available to all membrane users.

Key words | commercial membranes, dye removal, membrane characterization, nanofiltration

HIGHLIGHTS

- Commercial membranes have been characterized in detail.
- Its usability has been tested in textile wastewater treatment.
- A wide data set has been created.
- Figure of merits relation made in order to see the synergistic effect of many variable parameters on membrane performance more clearly.

Meltem Ağtaş
Başak Keskin
İsmail Koyuncu (corresponding author)
Department of Environmental Engineering,
Istanbul Technical University,
34467, Istanbul,
Turkey
E-mail: *koyuncu@itu.edu.tr*

Meltem Ağtaş
Başak Keskin
Türker Türken
İsmail Koyuncu
National Research Center on Membrane Technologies,
Istanbul Technical University,
Maslak, Istanbul,
Turkey

Türkan Ormancı-Acar
Faculty of Engineering, Department of Environmental Engineering,
Istanbul University-Cerrahpasa,
Istanbul,
Turkey

doi: 10.2166/wst.2021.125

GRAPHICAL ABSTRACT

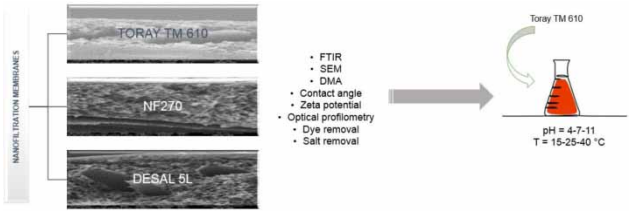

INTRODUCTION

Membrane technologies have reached an important point in the field of the environment in terms of pollution reduction and reuse of treated water. In particular, nanofiltration (NF) and reverse osmosis (RO) membranes are alternatives used in textile wastewater treatment because they provide high effluent quality (Barredo-Damas *et al.* 2006). NF membranes have lots of advantages when compared with ultrafiltration (UF) and RO membranes. For instance, NF membranes can be operated at lower pressure rates than RO membranes, but still have high retention of multivalent salts and other molecular compounds. As lower pressure rates are enough for NF membranes, operation, investment and maintenance costs are relatively minor (Lau & Ismail 2009).

The dyes used in the textile industry are highly harmful to aquatic life and the environment. Here, it is of great importance to treat the textile industry wastewater before being discharged (Lü *et al.* 2019). In addition, high amounts of water are used in processes in the textile industry. As groundwater is preferred as the source, the level of groundwater decreases and water recovery becomes important (Koyuncu 2002; Koyuncu *et al.* 2004). As conventional treatment methods cannot be always sufficient to meet discharge limits and considering water recovery (Ağtaş *et al.* 2020), membrane processes and nanofiltration membranes become prominent.

In recent years, many studies have been carried out on the treatment of textile wastewater using nanofiltration membranes. Babu and Murthy (Babu & Murthy 2017) coated polyethersulfone (PES) UF membranes with poly(vinyl alcohol) (PVA) and produced NF membranes. After fabrication of the NF membranes, performance was evaluated by cross-flow filtration using commercial textile dyes (acid, reactive and disperse). Maximum dye rejection of about 97.7% was observed for disperse dyes. In a very recent study (Tavangar *et al.* 2019), real textile wastewater was utilized and treated with electrocoagulation (EC) and NF membrane separately and with the combination of these two processes (EC-NF). NP010, Microdyn Nadir loose NF membranes was used with the aim of dye retention and salt permeability. After efficiency tests, it has been seen that NP010 commercial NF membranes showed effective refinement of dyes when it permeated inorganic salts and gave an opportunity to reuse salts and water. Kurt *et al.* (2012) used NF/RO commercial membranes in a pilot scale system to treat segregated wastewaters from dyewash processes in a weaving industry for decolorization, as well as the removal of chemical oxygen demand and salts. NF-270 was used for the nanofiltration process. Sufficient removal efficiency for dyes was obtained (Kurt *et al.* 2012).

Membrane morphology can be classified as one of the major parameters that have an effect on the membrane's performance. In order to understand the morphology of the membrane, there are methods and parameters commonly used for membrane characterization. For instance, pore size distribution, roughness, and contact angle are some of them. By measuring the contact angle of the membranes, the relationship between the membrane surface and the solution delivered to the membrane can be determined by looking at whether the membrane is hydrophilic or hydrophobic (Kwong *et al.* 2019; Schmidt *et al.* 2020). In the García-Fernández *et al.* (2017) study, to obtain optimal membrane structure for the membranes distillation process, alumina membranes were tested by using several membrane characterization techniques (García-fernández *et al.* 2017). In a recent study, it was aimed to constitute a meaningful relationship between oil retention and membrane structure by using network modeling. According to obtained results, it was reported that a network model is a significant device to understand membrane morphology's role in the treatment process (Li *et al.* 2019). When commercial membranes were used for treatment experiments, the information which is provided by the supplier cannot be

enough to foresee the rejection efficiencies of uncharged solutes. In Schmidt and friends' study, commercial membranes with different molecular weight cut-off (MWCO) values were tested and characterization of membranes was carried out by using atomic force microscopy and contact angle measurements. As a conclusion, it was stated that none of these parameters was associated with removal efficiency alone (Schmidt *et al.* 2020).

It can be understood from other publications that the membrane structure plays an important role on membrane performance. Therefore, the purpose of this study was to evaluate the effect of membrane properties on membrane performances. For this purpose, detailed analyses, which were Fourier transform infrared (FTIR) spectroscopy, scanning electron microscopy (SEM) analysis, optical profilometry, contact angle, mechanical strength (DMA) and zeta potential measurements were performed for each membrane (Toray TM 610, NF 270 and Desal 5 L). Additionally, pure water, two type of dyes (Setazol Red and Reactive Orange) filtration and salt removal tests were also carried out. Results were given in comparison with each other.

EXPERIMENTAL

Materials

Commercially available nanofiltration membranes Toray TM 610, NF 270 and Desal 5 L were purchased from Toray, Dow and Osmonics companies respectively.

Reactive Orange dye (mw: 617.54 g/mol) were purchased from Sigma-Aldrich, Ltd; $MgSO_4$ and NaCl were purchased from Tekkim Chemistry, Ltd; and Setazol Red reactive dye (Mw: 1,463 g/mol) was kindly supplied from Setas Chemicals, Tekirdağ, Turkey. Distilled water was used throughout this work.

Membrane characterization

The following experiments were conducted for the structural characterization of commercial NF membranes:

- Zeta potential analysis,
- FTIR analysis,
- Contact angle,
- Mechanical strength (DMA),
- SEM analysis,
- Surface roughness analysis with optical profilometer.

Surface charge of membranes was measured with electrokinetic analyzer (SurPAS, Anton Paar GmbH). To obtain the results of pH effect, pH value was changed between 4 and 11 during the analysis. Here, 1.0 mM KCl solution was used to circulate inside the adjustable gap cell containing membranes. The specific functional groups on the membrane surfaces were determined by FTIR (Spectrum 100, PerkinElmer, USA). The contact angle of the membranes was measured on an KSV Attension Theta contact angle device using a sessile drop technique on dried membranes. First, a small drop of distilled water is dropped onto the membrane surface using suitable equipment. Then, the contact angle device records the images of this water droplet on the membrane in a certain time interval for a total of 10 frames and calculates the contact angle. To ensure the accuracy of the measurement, the analyses were performed on four different locations on each membrane. The surface and cross-sections of membranes were scanned using SEM (Philips-XL30 SFEG) in high vacuum mode after coating with gold–palladium (Au–Pd). The roughness of the resulting membranes was determined by using 3D Optical Surface Profilers (Zygo New view 7100, Middlefield, CT).

Filtration experiments

Pure water flux performances of commercial NF membranes were investigated under four different pressures of 6, 9, 12 and 15 bar using distilled water. Performance tests were performed for NF membranes in the cross-flow system. The cross-flow system can be operated under both low (0–2 bar) and high (40–50 bar) pressure conditions. The system consisted of feed tank, feed pump, cartridge filter, membrane filtration cell, permeate tank, PLC panel, computer with supervisory control and data acquisition (SCADA), flow meter, and pressure, pH, temperature and conductivity sensors. The effective filtration area of the membrane in the membrane filtration cell was 155 cm^2 Other details on this system can be found in Kose-Mutlu *et al.*'s study (Kose-Mutlu *et al.* 2017).

Salt rejection performances of commercial NF membranes were performed using two types of salt solution as monovalent and divalent ions. Commercial membrane companies often use $MgSO_4$ to characterize NF membranes. It is also known that there is salinity in textile wastewater that contains dyes (Yaseen & Scholz 2019; Dupont 2021). Therefore $MgSO_4$ salt, which contains divalent ions and NaCl which contains monovalent ions was used. These were prepared at 2,000 ppm in both solutions and tested for one hour at four different pressures, 6, 9, 12, and 15 bar.

Reactive dyes are generally used in textile dyeing industries (Tomei *et al.* 2016). For this reason, model solutions prepared with two reactive dyes were used in the dye tests within the scope of this study. Molecular weight 1,463 g/mol Setazol Red and molecular weight 617.54 g/mol Reactive Orange dyes were prepared and used at 100 mg/L.

RESULTS AND DISCUSSION

Structural properties of NF membranes

Membrane surface roughness and functional groups in its structure are the main factors that affect water contact angle (Ang *et al.* 2020). Six different contact angle measurements were conducted with Toray TM 610, Desal 5 L and NF270 samples. Three of them were selected and an average contact angle was determined. The results are shown in Figure 1. As can be seen in the figure, the values obtained for NF membranes were found to be approximately 43, 9.5, and 28° for Toray, NF 270, and Desal 5 L membranes, respectively. When the graph was examined, it was seen that the contact angles of commercial NF membranes were quite low. This is thought to be due to the polyamide layer known to be hydrophilic.

The electrokinetic properties of the membrane revealed the electrical characteristics of the membrane surface. Measuring the potential difference in the liquid flow at the membrane surface at different pH ranges allowed us to measure the isoelectric point of the membrane surface. Understanding the effect of pH on surface load has a very important role in understanding the acid–base properties of functional groups on the membrane surface. The determination of the electrokinetic properties of membranes allowed to evaluate the operating conditions and chemical washing of the system. Furthermore, the effect of chemical washing agent on the membrane surface was evaluated by considering the results of the electrokinetic measurement. The method used in the experiments was the tangential liquid flow potential difference method, which enabled us to obtain information directly about the active layer of the membrane.

The zeta potentials of commercial NF membranes were measured at pH 4–12 and the zeta potential results are given in Figure 2. As can be seen from the figure, the zeta potentials of the membranes are negative. The reactive dyes used in the textile industry are negatively charged. In the Ormanci-Acar *et al.* (2018) study, Setazol Red and Reactive Orange dyes were used, which are same dyes used in our study. Zeta potentials were reported as −40 and −30 mV for Setazol Red and Reactive Orange dyes, respectively (Ormanci-Acar *et al.* 2018). So that the membrane surface was negative in order to prevent and minimize clogging. Because the dyes have better solubility at higher pH and better staining, the zeta potential at high pH is also very important. Commercial NF membranes are also negatively charged at −20 to −90 ranges.

Bonds on the surface of commercial NF membranes were determined by FTIR analysis. The peaks obtained are given in Figure 3.

As stated in Singh *et al.* (2014), according to their FTIR spectrum for polysulfone membrane, they observed 1,151 cm^{-1}, 1,244 cm^{-1} and 1,585 cm^{-1} peaks, which represented O–S–O stretching, C–O–C stretching and C–C aromatic bonds respectively and these bonds were apparent properties of sulfone group. In addition, for C–H stretching of the aromatic ring of polystyrene (PS), absorbances at 1,020 cm^{-1} and 830 cm^{-1} were also seen (Singh *et al.* 2014).

The commercial membranes examined had a strong peak at 1,584 cm^{-1}. It can be said that this peak represented a C=C bond, polysulfone and the weak peaks at 1,363 cm^{-1}

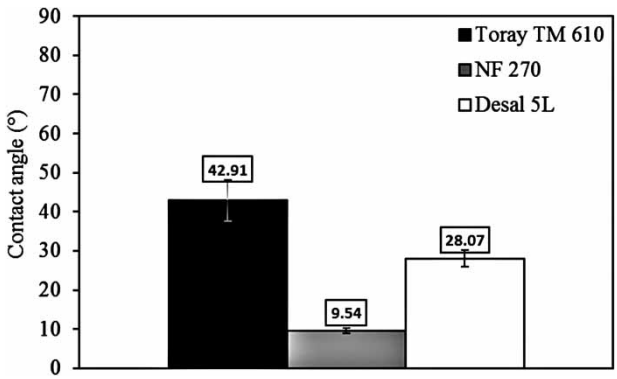

Figure 1 | Contact angle of commercial NF membranes.

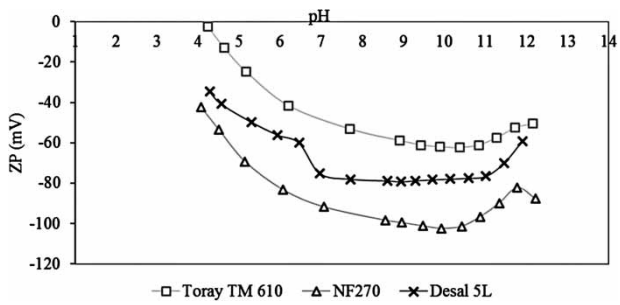

Figure 2 | Zeta potential of commercial NF membranes.

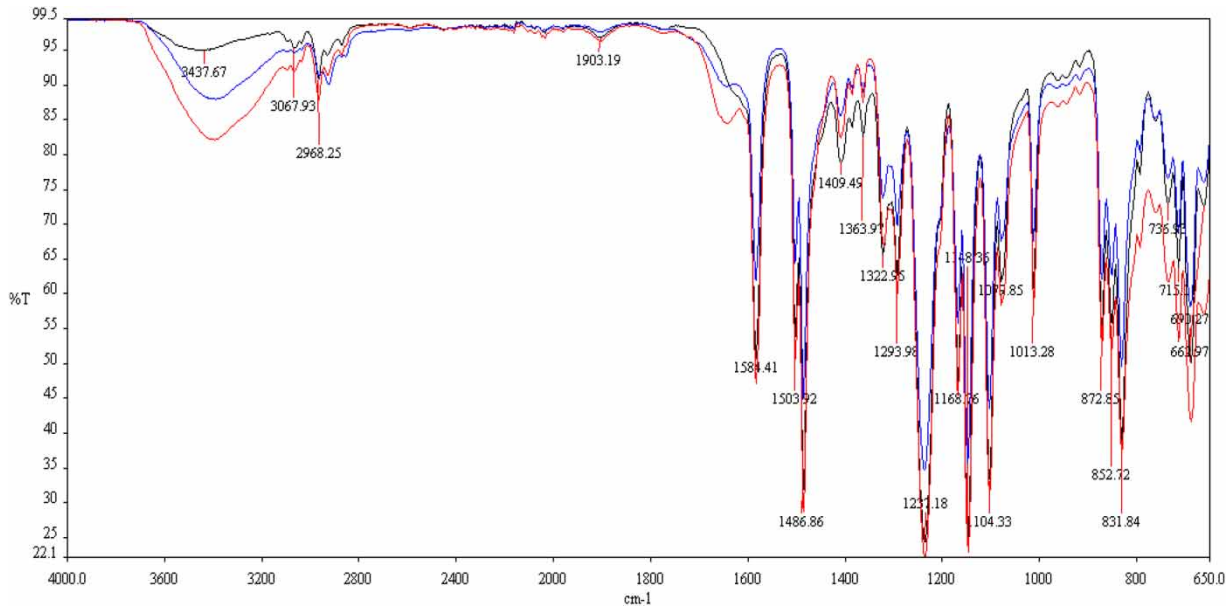

Figure 3 | FTIR results of commercial NF membranes (black line: Toray TM 610, blue line: NF270, red line: Desal 5 L). Please refer to the online version of this paper to see this figure in colour: http://dx.doi.org/10.2166/wst.2021.125.

were due to methyl groups (C–H bond bending in the alkene) (Puro *et al.* 2006). The peaks at 1,322 and 1,293 cm^{-1} were due to the asymmetric SO_2 stretch and the symmetrical SO_2 extension at 1,168 cm^{-1} (Puro *et al.* 2006). The peak present at 1,237 cm^{-1} showed an aryl-O-aryl extension. The large peak seen at 3,400 cm^{-1} showed some COOH groups in the thin film.

Young's modulus of the Toray TM 610, Desal 5 L and NF270 membranes is shown in Table 1. The highest Young's modulus was obtained with the Toray TM 610 membrane.

Roughness is important for membranes with thin film composite (TFC) coating. Because of the roughness of the membranes, this can prepare the ground for impurities to be retained on the membrane surface. When the surface roughness values of the commercial membranes were compared, it was seen that the lowest value was NF 270. This value also gives an idea about the quality of the surface coating. As indicated in Song's study, the polyamide active layer has unique surface properties that are called 'ridge-and-valley' conformation (Song *et al.* 2019). The surface roughness of each membrane is shown in Figure 4.

Table 1 | Mechanical properties of commercial NF membranes

	Toray TM610	NF270	Desal 5 L
Young's modulus, MPa	3.89	1.13	3.61
Elongation, %	15.01	22.17	4.56
Tensile force, N/mm^2	5.76	6.73	6.03

SEM images of commercial NF membranes are given in Figure 5. When the images were examined for Toray TM610, it is seen that it consists of a thin support layer. The voids in the support layer are believed to contain large macro-gaps. At the same time, surface roughness was observed when the surface images were examined. This indicated that pollutants with high concentrations can cling to the membrane surface and cause fouling. As stated in the Hobbs *et al.* (2006) study, when average roughness was increased, the flux decline ratio was also increased and this trend was attributed to increase in surface area which can lead to more area to which particles can adsorb (Hobbs *et al.* 2006). Vrijenhoek *et al.* (2001) also found that flux decline was more severe with the average roughness increase (Vrijenhoek *et al.* 2001).

Pure water flux performance of NF membranes

Pure water flux performances of commercial NF membranes under four different pressures, 6, 9, 12 and 15 bar, were investigated using distilled water. The results obtained with Toray TM 610, Desal 5 L and NF270 membranes are given in Figure 6. As seen from the figure, the lowest flux was obtained with Desal 5 L membrane. The results for Toray TM 610 and NF270 membranes were very close to each other.

Imbrogno & Schäfer (2019) also used NF270 for their study. They reported permeability of NF270 as 14 ± 2 $L/m^2.h.bar$ (Imbrogno & Schäfer 2019). To compare with our work, when this value is assumed as 16 $L/m^2.h.bar$;

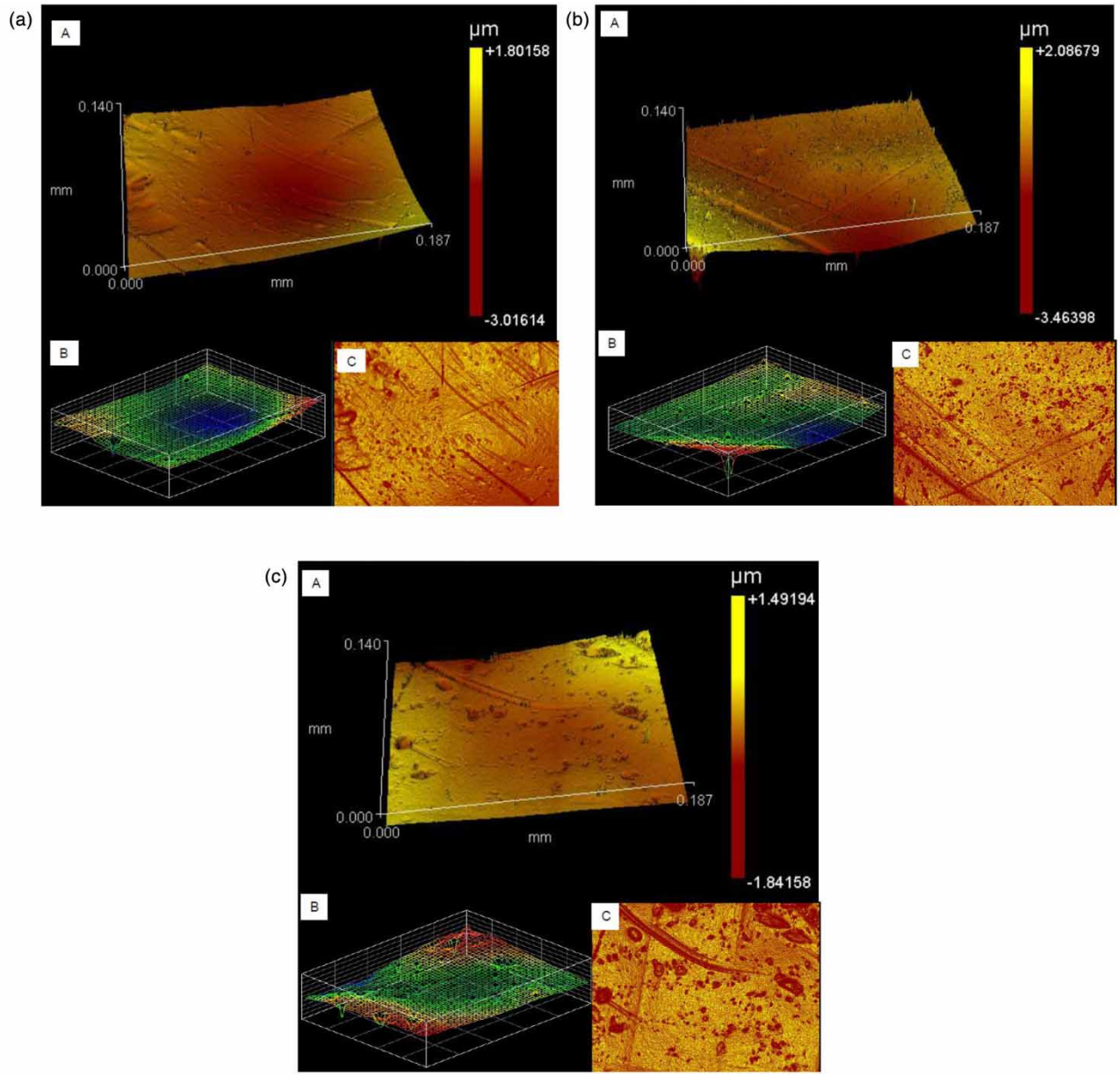

Figure 4 | Surface roughness of commercial membranes (a) Toray TM 610 (b) Desal 5 L (c) NF270 (A: 3D model, B:3D plot, C: solid plot).

96, 144, 192 and 240 L/m^2.h. values can be calculated for 6, 9, 12 and 15 bars, respectively. It can be seen that the values were compatible with each other.

Flux and rejection performance of NF membranes for $MgSO_4$ and NaCl solutions

Salt rejection performances of commercial NF membranes were performed using two types of salt solution as monovalent and divalent ions. $MgSO_4$ salt which contains divalent ions and NaCl which contains monovalent ions was used. They were prepared at 2,000 ppm in both solutions and tested for one hour at four different pressures, 6, 9, 12, 15 bar.

The salt retention performance of three different commercial membranes was investigated using 2,000 ppm $MgSO_4$ salt. The obtained flux results are shown in Figure 7 and the rejection efficiency results are given in Figure 8.

The best results were obtained with the Toray TM 610 membrane when considered as flux performance. Desal 5 L

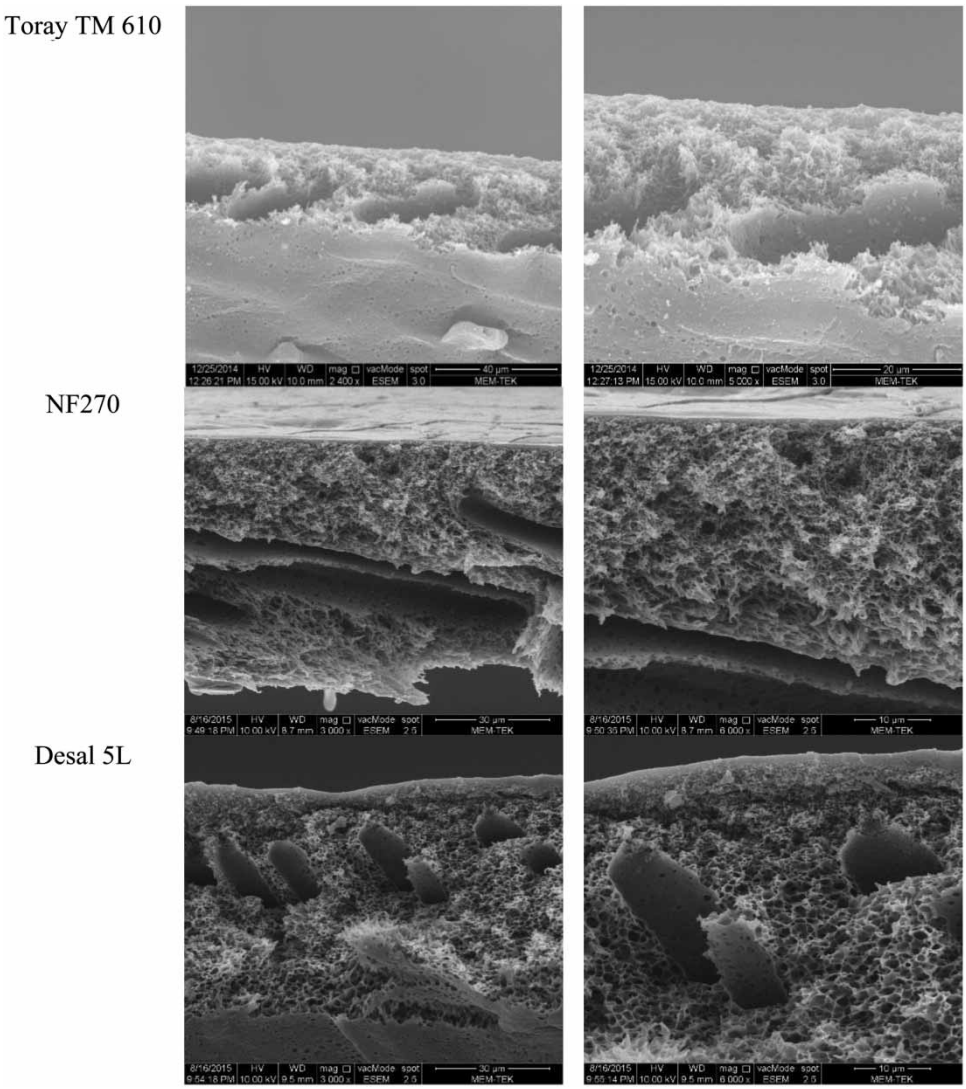

Figure 5 | SEM images of commercial membranes.

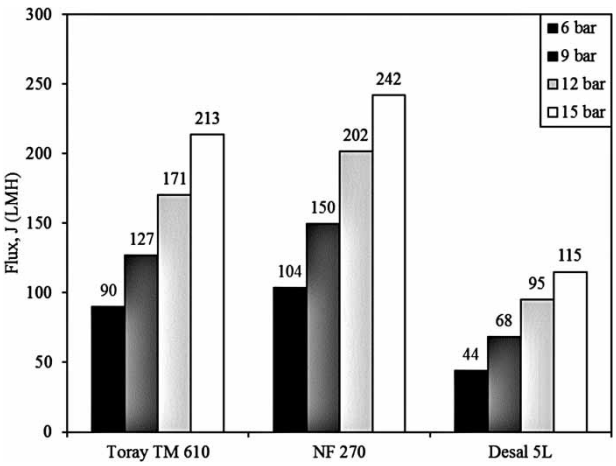

Figure 6 | Commercial NF membranes pure water flux values.

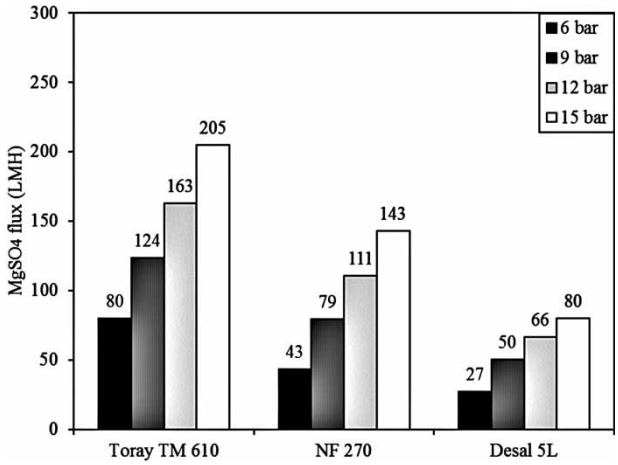

Figure 7 | $MgSO_4$ flux of commercial NF membranes.

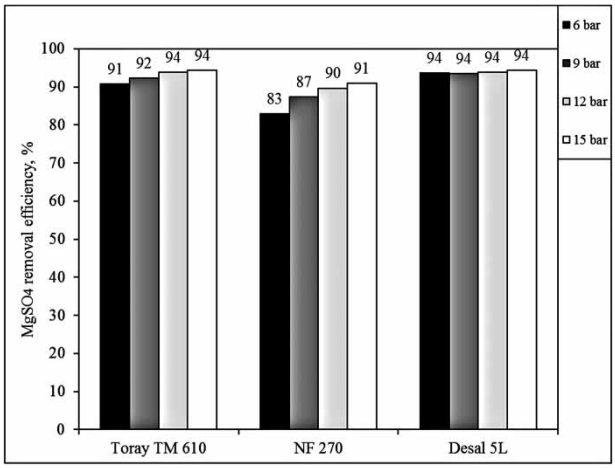

Figure 8 | $MgSO_4$ removal efficiency of commercial NF membranes.

and Toray TM 610 membranes, which provide the retention of magnesium salts around 94%, were particularly notable for the Toray's flux performance. Therefore, NaCl salt retention test and performance tests at different temperatures and at different pHs were performed using the Toray TM 610 membrane.

In a review study, salt rejection for the NF270 membrane is given. According to this information from the manufacturer in this review, salt rejection for NF270 membrane is reported as >97% (Mohammad *et al.* 2015). The same rejection rate also can be found in Abdel-Fatah's paper (Abdel-Fatah 2018). When the results were compared with our study, it can be said that they are not the same but have close values. This difference is thought to be due to the salt solution concentration or differences in the ambient conditions.

In Figure 9, $MgSO_4$ and NaCl salt removal efficiencies of Toray TM 610 membrane are given. As seen from the graph,

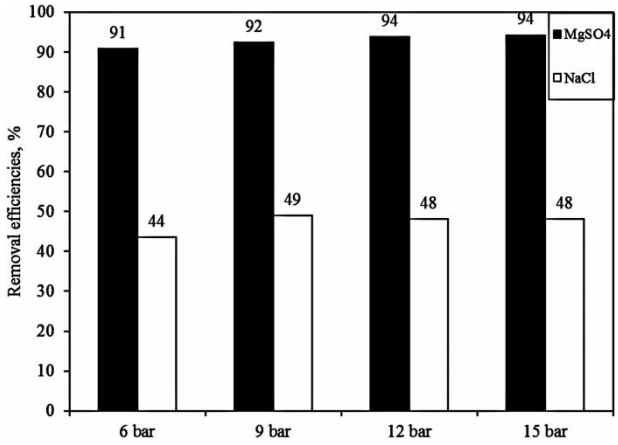

Figure 9 | $MgSO_4$ and NaCl removal efficiencies of Toray TM 610.

$MgSO_4$ removal efficiencies were almost twice the NaCl removal efficiencies. As $MgSO_4$ compound has divalent components, it is more likely that the Toray TM 610 membrane would retain $MgSO_4$ and permeate NaCl.

Flux and removal performance of NF membranes for dye solutions

Dye removal performance tests for the commercial Toray TM 610, NF 270 and Desal 5 L membrane are described in this section. Reactive dyes generally used in textile dyeing industries are preferred for this process. Molecular weight of 1,463 g/mol of Setazol Red and molecular weight 617.54 g/mol Reactive Orange dyes were prepared and used at 100 mg/L. Performance tests were also performed for NF membranes in the cross-flow system.

The Toray TM 610 membrane was selected from commercial NF membranes and dye performance tests were performed with the cross-flow system under 6, 9, 12, and 15 bar pressures. During the experiment, the dye solution was maintained at 25 °C and pH 8 (this pH is the normal pH of the dye solution).

Hourly flux data obtained by filtration of 100 mg/L Setazol Red dye for all membranes under four different pressures are given in Figure 10. As seen from the figure, the flux was fixed except for at 6 bars. Flux loss was observed at 6 bar. Figure 11 also gives Setazol Red dye removal performance. Removal efficiency of about 97–98% was achieved and performance increased as the pressure increased as expected.

The Reactive Orange removal efficiency with a lower molecular weight was also tested under the same conditions. The resulting flux changes are given in Figure 10. This figure shows that flux data are steadily progressing. In addition, it is seen that higher dye flux results were obtained as the Reactive Orange dye had a lower molecular weight compared to the reds obtained. Figure 11 also gives Reactive Orange dye removal efficiencies. High removal efficiencies of 96–99% were also obtained.

Flux and dye removal efficiency of Toray TM 610 under different pH and temperature values

The commercial NF membrane, which was tested under 6, 9, 12, and 15 bar pressures with pure water at 25 °C, was tested with pure water at 15 and 40 °C and the effects of temperature on flux were investigated. The flux data obtained under different pressures at these three different temperatures were compared in Figure 12. When this

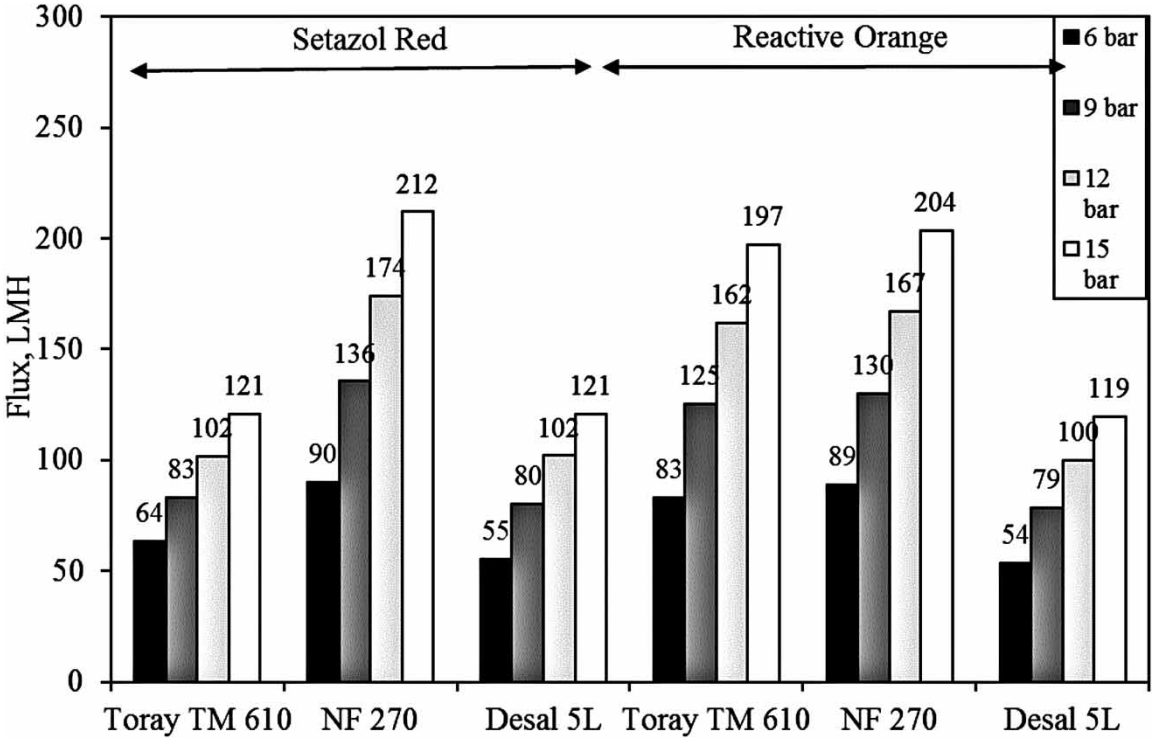

Figure 10 | Flux of NF commercial membranes for Setazol Red and Reactive Orange dye solutions.

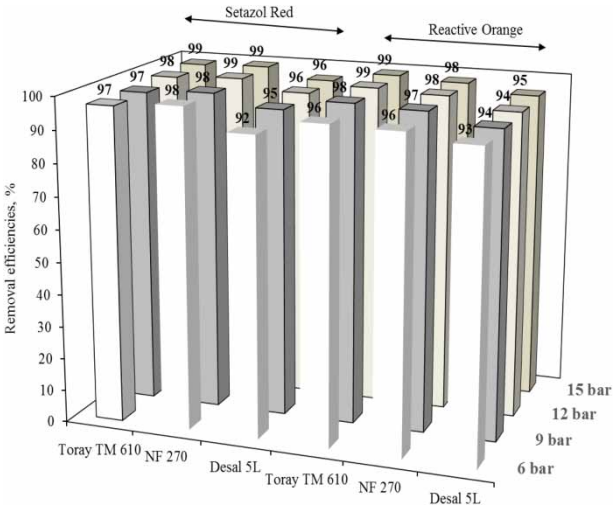

Figure 11 | Setazol Red and Reactive Orange dye removal efficiencies for NF commercial membranes.

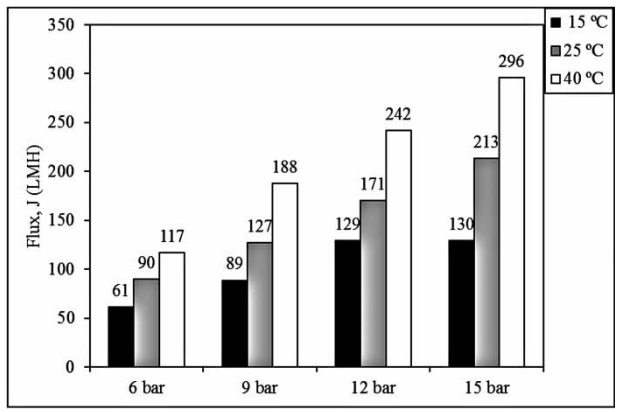

Figure 12 | Pure water flux of Toray TM 610 under different pressure and temperature values.

figure is examined, as expected, at the low temperature of 15 °C, flux had decreased and at 40 °C it had increased.

After observing that the temperature increased the flux, the effect on the dye removal efficiencies should also be examined. The dye performance of the commercial NF membranes (Toray TM 610) was also tested simultaneously at different temperatures and pH. For this, 100 mg/L Setazol Red and Reactive Orange dyes were prepared and tested at both 15 °C and 40 °C. Similarly, as the temperature increased, flux increase was observed with the Setazol Red dye.

Setazol Red flux changed due to pH at 15 °C and removal efficiencies are given in Tables 2 and 3. It is seen that pH increase did not change the flux significantly. It was observed that the removal efficiencies also increased at low and high pH levels.

Table 2 | Flux of Setazol Red and Reactive Orange solutions for different pH and temperature values for Toray TM 610 membrane

		15 °C			40 °C		
	Pressure (bar)	pH = 4	pH = 8	pH = 11	pH = 4	pH = 8	pH = 11
Flux of Setazol Red Solution (LMH)	6	61.9	68.0	51.7	71.4	93.5	81.3
	9	97.3	100.4	90.2	116.9	164.5	160.7
	12	123.7	122.4	125.5	156.0	209.3	232.1
	15	148.6	144.2	159.5	190.1	251.3	286.9
Flux of Reactive Orange Solution (LMH)	6	24.5	43.7	39.5	74.0	110.7	90.4
	9	43.6	68.9	73.3	117.5	173.9	158.4
	12	66.2	90.9	108.2	153.2	222.2	201.7
	15	95.2	118.7	149.4	179.2	272.9	243.3

Table 3 | Removal efficiencies of Setazol Red and Reactive Orange dye for different pH and temperature values for Toray TM 610 membrane

		15 °C			40 °C		
	Pressure (bar)	pH = 4	pH = 8	pH = 11	pH = 4	pH = 8	pH = 11
Setazol Red Removal Efficiency (%)	6	98.4	94.8	99.0	96.9	93.8	97.9
	9	98.6	92.3	99.0	98.0	91.2	98.2
	12	99.2	94.5	99.1	98.3	92.4	98.4
	15	99.3	90.1	99.4	98.6	93.5	98.6
Reactive Orange Removal Efficiency (%)	6	98.9	97.0	99.2	98.2	97.0	98.9
	9	99.1	99.0	99.3	98.8	99.0	99.4
	12	99.3	99.3	99.4	99.1	99.3	99.6
	15	99.3	99.3	99.6	99.2	99.3	99.5

The flux and removal efficiencies obtained at different pH at 15 °C for Reactive Orange dye are also given in Tables 2 and 3. An increase in efficiency was observed with the increase of pressure but the increase in pH did not affect the efficiencies. For 40 °C at different pHs, the highest flux was obtained at pH 8, but again the pH change did not significantly change the efficiency.

Effect of membrane properties on membrane performance

Within the scope of this study, three different commercial membranes were analyzed in detail and performance tests were carried out. In this section, the relationships that can be established between the structural properties and performances of membranes were investigated.

First of all, the graphic examining the results of surface roughness and $MgSO_4$ removal together is given in Figure 13. Desal 5 L, Toray TM 610 and NF 270 results are given as 5.54, 4.81 and 3.33 respectively. As can be seen from the graph, there is a linear relationship between surface roughness and salt removal efficiency. As the difference between the surface roughness values increases, the difference in removal efficiencies also increases. This can be attributed to increased membrane surface area due to increased surface roughness and more surface area where salt molecules can be adsorbed. As was also stated in the Ghiasi *et al.* (2019) study, when roughness is increased, an effective surface will be higher (Ghiasi *et al.* 2019).

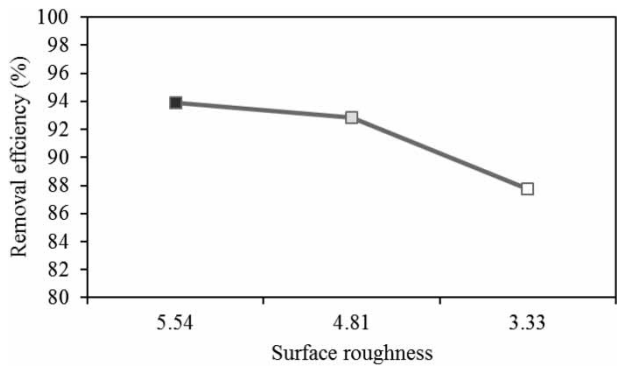

Figure 13 | Correlation between surface roughness and $MgSO_4$ removal.

When the contact angle values were analyzed, it was seen that the lowest value was on the NF270 membrane (see Figure 1). As previously published, as the contact angle decreases, the hydrophilicity of the membrane increases (Kajekar *et al.* 2015). It was reported in the Türken *et al.* (2015) study that bare membrane contact angle was 94° and for modified membranes was 69°. They indicated that modified membranes were more hydrophilic (Türken *et al.* 2015). Accordingly, it can be seen that the NF270 membrane had higher values than other membranes when looking at pure water and dye fluxes. The other two membranes, conversely, were not compatible with the correlation indicated. Although this is not an expected result, it is thought that when the contact angle and Young's modulus results are evaluated together, the following conclusion can be reached. When Young's modulus values were examined, the lowest value was for the NF270 membrane. The results of Toray and Desal membranes were very close to each other (see Table 1). As Young's modulus is a value that expresses the mechanical strength of the membrane and the NF270 membrane has the lowest result, it can be thought that pressure application will affect the NF270 membrane more severely than the other two commercial membranes and deform its pores. As in most industrial applications, high pressures are applied to the membranes, it is also stated in the article by Longo *et al.* (2018) that analysis of mechanical properties are important (Longo *et al.* 2018).

As mentioned in the previous section, dye removal tests at different pH and temperatures were applied to the Toray membrane and many results were obtained. In order to evaluate the membrane performance based on many parameters, to identify a holistic approach and to understand the results more easily, the method in the article of Sengur-Tasdemir *et al.* (2016) was tried to adapt to the results in this study (Sengur-Tasdemir *et al.* 2016). In order to apply this method, four different variables (dye removal efficiency, zeta potential, pH and temperature) that are thought to affect membrane performance were selected and normalized as figure of merits (FOM):

$$FOM = R_n Z_n P_n T_n$$

where FOM is the figure of merit, R_n is dye rejection, Z_n is zeta potential for pH values, P_n is pH and T_n is temperature. All of the obtained values were normalized by dividing them into the smallest value and the results are given in the Table 4.

When we look at the table, some points attract attention. First of all, when the relationship between pressure and FOM is evaluated, it is understood that there is no significant difference with pressure change. In particular, this can be clearly seen at the pH = 4 level for both dyes. At different pressures, all FOM values remained almost the same. Here, it can be concluded that pressure did not have any effect on performance value. The same result is also valid for the dye type. The dyes used in the study are dyes with different molecular weights. Despite this, although the dye type varied in the experiments, FOM values were not changed. When performance values at different temperatures are perused, it can be seen that the increase between the values for same pH values is in the form of a constant coefficient. To explain with an example, there is a constant 2.6 times change between the value at any pressure for a FOM of 15 °C pH = 4 and a FOM at 40 °C pH = 4. This also applies to other pH values. The reason for this is that the ratio of 40 to 15 is 2.6. Therefore, the temperature value functions as a constant coefficient in

Table 4 | Figure of merits of Toray TM 610 NF membrane

		15 °C			40 °C		
	Pressure (bar)	**pH = 4**	**pH = 8**	**pH = 11**	**pH = 4**	**pH = 8**	**pH = 11**
6	Setazol Red	1.00	52.99	78.85	2.63	139.81	207.94
9		1.00	51.59	78.85	2.66	135.93	208.58
12		1.01	52.82	78.93	2.66	137.72	209.00
15		1.01	50.36	79.17	2.67	139.36	209.42
6	Reactive Orange	1.01	54.22	79.01	2.66	144.58	210.06
9		1.01	55.34	79.09	2.68	147.56	211.12
12		1.01	55.50	79.17	2.69	148.01	211.55
15		1.01	55.50	79.33	2.69	148.01	211.36

this equation. As a result, it can be concluded that the temperature difference did not have a meaningful impact on performance.

To determine surface charge of membranes, zeta potential can be used as an essential and credible indicator (Cheng *et al.* 2016). Zeta potential is a method that determines the charge of the membrane surface at different pH in general (Kajekar *et al.* 2015). In the experiments carried out within the scope of this study, the surface charge of the Toray membrane at different pH was determined. When the surface charge of the Toray membrane was close to the isoelectric point at pH = 4, it became more and more negative as the pH was increased (see Figure 2). As dye solutions used in the experiments had a negative charge, it can be thought that this will provide removal with the repulsive force that will occur between the membrane and the dye solution. Based on this mechanism, when the zeta potential at pH = 4 is close to 0, it was thought that the dye was adsorbed on the membrane surface rather than undergoing repulsive forces. As the pH value was increased, the reason for the removal efficiency passed from adsorption to repulsive forces. Therefore, it was concluded that the two most important parameters affecting performance were zeta potential and pH.

CONCLUSION

This study compared the performance and membrane characteristics of three commercial nanofiltration membranes (Toray TM 610, NF 270 and Desal 5 L) for treatment of dye and salt solutions. After pure water and dye removal tests, the Toray TM 610 membrane was selected and under different pH (pH = 4–7–11) and temperature values (T = 15, 25 and 40 °C) dye removal tests were repeated for Toray TM 610. According to membranes characterization tests, it can be seen that all of the commercial NF membranes tended to be hydrophilic and their surface was negative in general. The hydrophilicity of the membrane surface is known as a flux-enhancing parameter. Furthermore, the negative surface of the membrane can prevent membrane fouling due to the generally negative nature of the dyes. According to the results obtained, the importance of contact angle, mechanical strength and surface roughness is underlined. It was concluded that the most important properties for dye removal performance is zeta potential. It is thought that this study may provide a starting point for other studies.

ACKNOWLEDGEMENTS

This work was supported by the Scientific and Technological Research Council of Turkey (TUBİTAK). Project number: 113Y371.

DECLARATION OF INTERESTS

The authors declare that they have no known competing financial interests or personal relationships that could have appeared to influence the work reported in this paper.

DATA AVAILABILITY STATEMENT

All relevant data are included in the paper or its Supplementary Information.

REFERENCES

Abdel-Fatah, M. A. 2018 Nanofiltration systems and applications in wastewater treatment: review article. *Ain Shams Engineering Journal* **9** (4), 3077–3092. https://doi.org/10.1016/j.asej.2018.08.001.

Ağtaş, M., Yılmaz, Ö., Dilaver, M., Alp, K. & Koyuncu, İ. 2020 Hot water recovery and reuse in textile sector with pilot scale ceramic ultrafiltration/nanofiltration membrane system. *Journal of Cleaner Production* **256**, 120359.

Ang, M. B. M. Y., Tang, C. L., De Guzman, M. R., Maganto, H. L. C., Caparanga, A. R., Huang, S. H., Tsai, H. A., Hu, C. C., Lee, K. R. & Lai, J. Y. 2020 Improved performance of thin-film nanofiltration membranes fabricated with the intervention of surfactants having different structures for water treatment. *Desalination* **481**, 114352.

Babu, J. & Murthy, Z. V. P. 2017 Treatment of textile dyes containing wastewaters with PES/PVA thin film composite nanofiltration membranes. *Separation and Purification Technology* **183**, 66–72. http://dx.doi.org/10.1016/j.seppur.2017.04.002.

Barredo-Damas, S., Alcaina-Miranda, M. I., Iborra-Clar, M. I., Bes-Piá, A., Mendoza-Roca, J. A. & Iborra-Clar, A. 2006 Study of the UF process as pretreatment of NF membranes for textile wastewater reuse. *Desalination* **200** (1–3), 745–747.

Cheng, X., Li, N., Zhu, M., Zhang, L., Deng, Y. & Deng, C. 2016 Positively charged microporous ceramic membrane for the removal of Titan Yellow through electrostatic adsorption. *Journal of Environmental Sciences (China)* **44**, 204–212.

Dupont 2021 FilmTec™ Membranes **9**(45), 3–5. https://www.dupont.com/brands/filmtec.html.

García-fernández, L., Wang, B., García-payo, M. C., Li, K. & Khayet, M. 2017 Morphological design of alumina hollow

fiber membranes for desalination by air gap membrane distillation. *Desalination* **420**, 226–240.

Ghiasi, S., Behboudi, A., Mohammadi, T. & Khanlari, S. 2019 Effect of surface charge and roughness on ultrafiltration membranes performance and polyelectrolyte nanofiltration layer assembly. *Colloids and Surfaces A: Physicochemical and Engineering Aspects* **580**, 123753. https://doi.org/10.1016/j.colsurfa.2019.123753.

Hobbs, C., Hong, S. & Taylor, J. 2006 Effect of surface roughness on fouling of RO and NF membranes during filtration of a high organic surficial groundwater. *Journal of Water Supply: Research and Technology – AQUA* **55** (7–8), 559–570.

Imbrogno, A. & Schäfer, A. I. 2019 Comparative study of nanofiltration membrane characterization devices of different dimension and configuration (cross flow and dead end). *Journal of Membrane Science* **585**, 67–80. https://doi.org/10.1016/j.memsci.2019.04.035.

Kajekar, A. J., Dodamani, B. M., Isloor, A. M., Karim, Z. A., Cheer, N. B., Ismail, A. F. & Shilton, S. J. 2015 Preparation and characterization of novel PSf/PVP/PANI-nanofiber nanocomposite hollow fiber ultrafiltration membranes and their possible applications for hazardous dye rejection. *Desalination* **365**, 117–125.

Kose-Mutlu, B., Ersahin, M. E., Ozgun, H., Kaya, R., Kinaci, C. & Koyuncu, I. 2017 Influence of powdered and granular activated carbon system as a pre-treatment alternative for membrane filtration of produced water. *Journal of Chemical Technology and Biotechnology* **92** (2), 283–291.

Koyuncu, I. 2002 Reactive dye removal in dye/salt mixtures by nanofiltration membranes containing vinylsulphone dyes: effects of feed concentration and cross flow velocity. *Desalination* **143**, 243–253.

Koyuncu, I., Topacik, D. & Wiesner, M. R. 2004 Factors influencing flux decline during nanofiltration of solutions containing dyes and salts. *Water Research* **38** (2), 432–440.

Kurt, E., Koseoglu-imer, D. Y., Dizge, N., Chellam, S. & Koyuncu, I. 2012 Pilot-scale evaluation of nano fi ltration and reverse osmosis for process reuse of segregated textile dyewash wastewater. *DES* **302**, 24–32. http://dx.doi.org/10.1016/j.desal.2012.05.019.

Kwong, M., Abdelrasoul, A. & Doan, H. 2019 Results in materials controlling polysulfone (PSF) fiber diameter and membrane morphology for an enhanced ultrafiltration performance using heat treatment. *Results in Materials* **2**, 100021. https://doi.org/10.1016/j.rinma.2019.100021.

Lau, W. J. & Ismail, A. F. 2009 Polymeric nanofiltration membranes for textile dye wastewater treatment: preparation, performance evaluation, transport modelling, and fouling control – a review. *Desalination* **245** (1–3), 321–348.

Li, Z., Liu, X., Chen, G., Deng, B. & Li, W. 2019 Effects of membrane morphology on the rejection of oil droplets: theoretical analysis based on network modeling. *Journal of Membrane Science* **588**, 117198.

Longo, M., De Santo, M. P., Esposito, E., Fuoco, A., Monteleone, M., Giorno, L. & Jansen, J. C. 2018 Force spectroscopy determination of Young's modulus in mixed matrix membranes. *Polymer* **156**, 22–29. https://doi.org/10.1016/j.polymer.2018.09.043.

Lü, Z., Hu, F., Li, H., Zhang, X., Yu, S., Liu, M. & Gao, C. 2019 Composite nanofiltration membrane with asymmetric selective separation layer for enhanced separation efficiency to anionic dye aqueous solution. *Journal of Hazardous Materials* **368**, 436–443. https://doi.org/10.1016/j.jhazmat.2019.01.086.

Mohammad, A. W., Teow, Y. H., Ang, W. L., Chung, Y. T., Oatley-Radcliffe, D. L. & Hilal, N. 2015 Nanofiltration membranes review: recent advances and future prospects. *Desalination* **356**, 226–254. http://dx.doi.org/10.1016/j.desal.2014.10.043.

Ormanci-Acar, T., Celebi, F., Keskin, B., Mutlu-Salmanlı, O., Agtas, M., Turken, T., Tufani, A., Imer, D. Y., Ince, G. O., Demir, T. U., Menceloglu, Y. Z., Unal, S. & Koyuncu, I. 2018 Fabrication and characterization of temperature and pH resistant thin film nanocomposite membranes embedded with halloysite nanotubes for dye rejection. *Desalination* **429**, 20–32.

Puro, L., Mänttäri, M., Pihlajamäki, A. & Nyström, M. 2006 Characterization of modified nanofiltration membranes by octanoic acid permeation and FTIR analysis. *Chemical Engineering Research and Design* **84** (2A), 87–96.

Schmidt, C. M., Sprunk, M., Löffler, R. & Hinrichs, J. 2020 Relating nanofiltration membrane morphology to observed rejection of saccharides. *Separation and Purification Technology* **239**, 116550. https://doi.org/10.1016/j.seppur.2020.116550.

Sengur-Tasdemir, R., Urper, G. M., Turken, T., Genceli, E. A., Tarabara, V. V. & Koyuncu, I. 2016 Combined effects of hollow fiber fabrication conditions and casting mixture composition on the properties of polysulfone ultrafiltration membranes. *Separation Science and Technology (Philadelphia)* **51** (12), 2070–2079. http://dx.doi.org/10.1080/01496395.2016.1198811.

Singh, K., Devi, S., Bajaj, H. C., Ingole, P., Choudhari, J. & Bhrambhatt, H. 2014 Optical resolution of racemic mixtures of amino acids through nanofiltration membrane process. *Separation Science and Technology (Philadelphia)* **49** (17), 2630–2641. http://dx.doi.org/10.1080/01496395.2014.911023.

Song, X., Gan, B., Yang, Z., Tang, C. Y. & Gao, C. 2019 Confined nanobubbles shape the surface roughness structures of thin film composite polyamide desalination membranes. *Journal of Membrane Science* **582**, 342–349. https://doi.org/10.1016/j.memsci.2019.04.027.

Tavangar, T., Jalali, K., Alaei Shahmirzadi, M. A. & Karimi, M. 2019 Toward real textile wastewater treatment: membrane fouling control and effective fractionation of dyes/inorganic salts using a hybrid electrocoagulation – nanofiltration process. *Separation and Purification Technology* **216**, 115–125.

Tomei, M. C., Soria Pascual, J. & Mosca Angelucci, D. 2016 Analysing performance of real textile wastewater bio-decolourization under different reaction environments. *Journal of Cleaner Production* **129**, 468–477. http://dx.doi.org/10.1016/j.jclepro.2016.04.028.

Türken, T., Sengur-Tasdemir, R., Koseoglu-Imer, D. Y. & Koyuncu, I. 2015 Determination of filtration performances of nanocomposite hollow fiber membranes with silver nanoparticles. *Environmental Engineering Science* **32** (8), 656–665.

Vrijenhoek, E. M., Hong, S. & Elimelech, M. 2001 Influence of membrane surface properties on initial rate of colloidal fouling of reverse osmosis and nanofiltration membranes. *Journal of Membrane Science* **188** (1), 115–128.

Yaseen, D. A. & Scholz, M. 2019 *Textile Dye Wastewater Characteristics and Constituents of Synthetic Effluents: A Critical Review*. Springer, Berlin, Heidelberg.

First received 30 December 2020; accepted in revised form 22 March 2021. Available online 29 March 2021